Reliability Engineering and System Safety 225 (2022) 108630

Contents lists available at ScienceDirect

Reliability Engineering and System Safety

journal homepage: www.elsevier.com/locate/ress

Multifractional and long-range dependent characteristics for remaining useful life prediction of cracking gas compressor

Wanqing Song [a,*], Shouwu Duan [b], Enrico Zio [3], Aleksey Kudreyko [d]

[a] School of Electronic and Electrical Engineering, Minnan University of Science and Technology, Quanzhou 362700, China
[b] School of Electronic & Electrical Engineering, Shanghai University of Engineering Science, Shanghai, 201620, China
[c] Energy Department, Politecnico di Milano, Via La Masa 34/3, 20156, Italy
[d] Department of Medical Physics and Computer Science, Bashkir State Medical University, Lenina st. 3, 450008 Ufa, Russia

ARTICLE INFO

Keywords:
Cracking gas compressor
Remaining useful life
Linear multifractional Levy stable motion
Long-range dependence
Non-Gaussian

ABSTRACT

Cracking gas compressor (CGC) is a complex equipment used in ethylene production facilities. For the reliable and safe operation of CGC, the prediction of its remaining useful life (RUL) of relevance. The degradation process of a CGC from a normal state to a failure state has long-range dependence (LRD) with nonlinear and multifractal features. Concurrently, the increment of the degradation process obeys a non-Gaussian distribution. In this study, a degradation model for RUL prediction of CGC is developed. The model is based on a nonlinear drift function and Linear Multifractional Levy Stable Motion (LMSM). The drift function describes the nonlinear characteristics of the degradation process, whereas the LMSM allows accounting for its LRD, multifractal and non-Gaussian characteristics. The LRD features reflect the slowness of the degradation process, the multifractional features allow capturing local irregularities due to degenerate data fluctuations, and can specifically describe degenerate sequences. Finally, a RUL prediction framework for CGC is proposed and, then, verified with real observation data collected from an operating CGC.

1. Introduction

1.1. Background and significance of work

Cracked-gas compressor is one of the most critical components of ethylene plants [1]. During the operation of CGC, various problems might be encountered, including coking caused by unsaturated hydrocarbon polymerization, erosion and wear of high-pressure separators, corrosion and leakage of sealing balance pipe flange, turbine scaling etc. [2,3]. These problems can lead to ethylene production shutdown and even casualties. Currently, the CGC is equipped with various sensors to monitor temperature, pressure, flow, liquid level and other parameters. These parameters are not only used on-site for process monitoring and control, but can also be transmitted to the control center for the elaboration for detecting process anomalies and for predicting anomalous patterns trends. When these parameters exceed certain threshold values, the interlocking shutdown is activated to prevent CGC failure [4,5]. In this context, accurate prediction of RUL can be used to effectivity guide system pre-maintenance for increasing CGC reliability and safety of operation [6].

1.2. Literature review of statistical model-based approaches

A model is used to describe the uncertainty of the CGC degradation process and its effect on RUL prediction [7]. The statistical model-based approach amounts to fitting observed values onto the random process model to estimate its parameters. The variance of the model parameters describes the uncertainty caused by the limited statistics [8].

A degradation model with random coefficients has been used to predict the uncertainty in mechanical degradation [9,10]. The Gamma process model [11,12] has also been used, where the increments of the degenerate process at disjoint time intervals are assumed independent random variables following a Gamma distribution. The Wiener process model [13–15] is expressed as a drift term plus a diffusion term driven by Brownian motion, and has been used in stochastic degradation process models. The Inverse Gaussian process model [16,17] assumes that mechanical degradation processes have independent increments and follow an Inverse Gaussian distribution. A Markov model [18,19] assumes that the mechanical degradation process transitions occur in a in finite state space and according to the Markov property. All these models refer to a particular distribution, and have the Markov property: future states depend only on the current state, independent of past behavior.

* Corresponding author.
E-mail address: swqls@126.ceom (W. Song).

https://doi.org/10.1016/j.ress.2022.108630
Received 3 January 2022; Received in revised form 21 May 2022; Accepted 25 May 2022
Available online 28 May 2022

Acronyms and Abbreviations

CGC	Cracking Gas Compressor
FBM	Fractional Brownian Motion
GC	Generalized Cauchy
HD	Health Degree
LFSM	Linear Fractional Levy Motion
LMSM	Linear Multifractional Levy Stable Motion
LSTM	Long Short-Term Memory
LRD	Long-Range Dependence
MAPE	Mean Absolute Percentage Error
PDF	Probability Density Function
RMSE	Root Mean Square Error
RUL	Remaining Useful Life
SOA	Score of Accuracy

However, this property is not always valid in practical applications.

Non-Markov models reflect the fact that the future state not only depends on the current state, but it is related to previous states, that is, the Long-Range dependence (LRD) feature. Gaussian and non-Gaussian models can be developed according to the probability distribution of the random noise in the model. The Gaussian models assume that the noise distribution obeys normal distribution. Such models include the generalized Cauchy method (GC) [20,21] and the fractional Brownian motion (FBM) models [22,23]. The models are limited to the degradation process with small fluctuation range of data and are not valid for the heavy tail phenomenon. The non-Gaussian linear fractional Levy motion (LFSM) models [24,25], on the contrary, allow capturing the heavy-tail characteristics in the degradation process tail parameter α. However, LFSM is a phenomenon of global irregularity characterized by a constant Hurst index. In addition, LSTM recurrent neural network (RNN) [26,27] also has LRD characteristics, but LSTM-RNN, like any neural network, needs sufficient data for training.

1.3. Formulation of the problem of interest for this study

In practice, operating conditions and ambient noise will inevitably change in time. Some researchers have carried out research on RUL prediction for equipment with changing operating conditions, such as the relaxation effect of battery [28,29], slag skin effect of blast furnace [30,31], dynamic operation of heavy machine tools [32], etc. The CGC operating conditions remain the same but the external environmental noise changes, so the degradation process trend changes due to the changes of operating conditions leading to local irregularities in the fluctuations. For more realistic modeling, a degradation model driven by LMSM [33,34,35] is proposed to predict the local irregular characteristics of the CGC degradation process. LMSM has LRD [36] and non-Gaussian characteristics. The LRD feature takes into account the time slowness of the CGC degradation process and the non-Gaussian feature describes the high jumps in data fluctuation of the CGC degradation process. In addition, When the tail parameter $\alpha = 2$, the LMSM model degenerates into a Gaussian model and when the tail parameter $0 < \alpha < 2$, LMSM is a non-Gaussian model. Therefore, the LFSM model can be flexibly applied to different situations according to the value of the tail parameter α [37].

1.4. Contributions

For the RUL prediction of CGC, a degradation model driven by the nonlinear drift function and LMSM diffusion term is developed. The nonlinear drift function predicts the nonlinear deterministic global trend and the LMSM describes the LRD, multifractal and non-Gaussian characteristics of the degradation process. The specific contributions of the work presented in the paper are as follows: the multifractional, LRD and non-Gaussian characteristics of LMSM are proved. Through the definition of derivability, it is deduced that the multifractional characteristic of a LMSM sequence is determined by both global $\min_{t\in I} H(t) - \frac{1}{\alpha}$ and local variables $H(t_0) - \frac{1}{\alpha}$; the ability to describe the local irregularity of degenerate processes is proved; based on whether the integral kernel of LMSM is a constant, the LRD condition is deduced as $H(t) > \frac{1}{\alpha}$; finally, the integral form of LMSM is discretized and, according to the stability law [38], LMSM is shown to obey Levy stable distribution and have non-Gaussian characteristic.

To calculate the RUL of the CGC, the following work is done. Firstly, the self-similar parameters of LMSM are derived by self-similar definition [39]. Secondly, according to the self-similar parameters, Maruyama Parameter [40] and Levy linear operation rules [41], the specific form of incremental distribution of LMSM degradation model is derived. Finally, because there is no explicit probability density function (PDF) expression for Levy stable distribution [42], RUL cannot be calculated using the weak convergence definition [43,44]. Then, based on Monte Carlo simulation [45] and previous derivations, this paper proposes an algorithm to calculate the RUL of a CGC.

1.5. Practical application and organization

For the practical application of RUL prediction of a CGC, a prediction framework is proposed in this paper. First, the parameter value sequences with predictability and LRD characteristics are screened from the data collected by the sensors. The maximum Lyapunov index and LRD conditions are used to judge the predictability and LRD characteristics of the collected data. When the maximum Lyapunov exponent is greater than 0, the data can be considered as predictable [46]; when Hurst exponent $H(t)$ and tail parameter α meet the condition $H(t) > \frac{1}{\alpha}$, the process is considered to have LRD characteristics. Secondly, the health indicators of CGC are constructed by using the selected parameter sequences. Methods such as Root Mean Square [47], Crest Factor [48] and Skip-over Factor [49] can be used to construct health indicators. Thirdly, the health indicator state is divided into normal process, degradation process and failure state. Note that the data from the degradation process is used to build subsequent degradation models. The other steps are parameter estimation, iterative degradation model establishment and RUL prediction.

To further verify the superiority of the model, it is compared with GC process [20,21], FBM [22,23], LFSM [24,25] and Long short-term Memory (LSTM) Recurrent Neural Network [26,27]. The Score of Accuracy (SOA), Health Degree (HD), Root Mean Square Error (RMSE) and Mean Absolute Percentage Error (MAPE) [50,51] are used for comparative error analysis.

The structure of this paper is as follows. In the second section, LMSM is introduced and its LRD, multifractional and non-Gaussian characteristics are analyzed. These characteristics already justify the superior realism of LMSM in prediction modeling. In Section 3, the degradation model driven by a nonlinear drift function and LMSM is developed, and the algorithm of RUL prediction is given. In Section 4, the parameters in the degradation model are estimated, where the Hurst function $H(t)$ is estimated with consistent and strongly consistent estimates, which does not require searching for sharp estimates of covariance related to the variogram. In the fifth section, the CGC fault event of Shanghai Secco Petrochemical Co., LTD is analyzed and RUL prediction is carried out. We, then, conclude the paper in the last section.

2. Linear multifractional Levy stable motion

The LFSM stochastic process can be defined by the following stochastic integral [24,25]:

$$X(t)=\int_{-\infty}^{\infty}\left\{\left[(t-s)_{+}^{H-\frac{1}{\alpha}}-(-s)_{+}^{H-\frac{1}{\alpha}}\right]+\left[(t-s)_{-}^{H-\frac{1}{\alpha}}-(-s)_{-}^{H-\frac{1}{\alpha}}\right]\right\}M(ds) \tag{1}$$

where $(t-s)_+=\max(t-s,0),(-s)_-=\max(s,0)$ and H is the self-similar parameter. $M(ds)$ is a cluster of symmetric Levy stable random variables. However, LFSM has limitations, which can only describe the phenomenon of uniform irregularity characterized by a single fractal structure or a constant Hurst exponent. For more realistic modeling, local variations of irregularity need to be considered, allowing the Holder exponent to vary from time to time or space. One way to achieve this generalization is to extend the standard LFSM to LMSM by the time function $H(t)$ exponential index [33]:

$$X(t,\ H(t))=\int_{-\infty}^{\infty}\left\{\left[(t-s)_{+}^{H(t)-\frac{1}{\alpha}}-(-s)_{+}^{H(t)-\frac{1}{\alpha}}\right]+\left[(t-s)_{-}^{H(t)-\frac{1}{\alpha}}-(-s)_{-}^{H(t)-\frac{1}{\alpha}}\right]\right\}M(ds) \tag{2}$$

where the tail parameter α determines the heavy-tailed degree of LMSM.

2.1. Differentiable and multifractional characteristics

Let us consider path continuity and roughness of LMSM. Observe that LMSM with $H(t)\ \leq 1/\alpha$ does not have continuous paths, i.e. paths that are continuous functions and satisfy several other nice properties [34]. A quite useful one among them, is that, for all fixed compact intervals $H(t)\in\left(\frac{1}{\alpha},1\right), t\in R$, the paths $X(t,\ H(t))$ has:

$$\sup\left\{\left|\frac{X(t_1,\ H(t_1))-X(t_2,\ H(t_2))}{t_1-t_1}\right|\right\}<+\infty,\ t_1,t_2\in t \tag{3}$$

where $H(t)$ is a continuous function. For any $t_1,t_2,$ the $H(t)$ has [22] :

$$\frac{|H(t_1)-H(t_2)|}{|t_1-t_2|^{\rho_H}}\leq c\ with\ \rho_H=\min_{t_1,t_2\in t}H(t)-\ \frac{1}{\alpha} \tag{4}$$

where c is the constant, and with the convention that $\left(\frac{0}{0}\right)\ =0$. It is clear that the LMSM $\{X(t,\ H(t))\ :\ t\ \in\ R\}$has continuous paths as long as its parameter $H(t)$ is a continuous function with values in $\left(\frac{1}{\alpha},\ 1\right)$ Obviously, as long as the parameter $H(t)$ in LMSM is a continuous function in the range of $\left(\frac{1}{\alpha},\ 1\right)$, then LMSM has a continuous path. It is possible to use stochastic differentiation to build a prediction model. We now turn to path irregularity of LMSM, which can classically be measured through Holder exponents [35]. Recall that for each nonempty continuous interval $\in R$, and every $\gamma\ \in[0,\ 1]$, for any $t_1,t_2,$ the Holder space $C_\gamma(I)$ is defined as:

$$C_\gamma(I)=\left\{f:I\in R:\ \sup_{t_1,t_2\in I}\left\{\ \frac{|f(t_1)-f(t_2)|}{|t_1-t_2|^{\gamma}}\right\}<+\infty\right\} \tag{5}$$

Let us define a global Holder exponent $\rho_g^{gobal}(I)$ over I:

$$\rho_g^{gobal}(I)=\sup\{\gamma\in[0,1]:g\in C_\gamma(I)\} \tag{6}$$

In the same way, the local Holder exponent $\rho_g^{local}(t_0)$ at an arbitrary $t_0\in\ R$ is:

$$\rho_g^{local}(t_0)=\sup\left\{\rho_g^{gobal}([M_1\ M_2]):M_1<t_0<M_2\right\} \tag{7}$$

when the continuous function g is LMSM $X(t,\ H(t))$, these two exponents are denoted by $\rho_X^{gobal}(I),\ \rho_X^{local}(t_0)$, respectively. According to Eqs. (3), (4) and (5), we can get:

$$\sup_{t_1,t_2\in I}\left\{\frac{|X(t_1,\ H(t_1))-X(t_2,\ H(t_2))|}{|t_1-t_2|^{\min_{t_1,t_2\in I}H(I)-\ \frac{1}{\alpha}}}\right\}<+\infty \tag{8}$$

Then, according to Eqs. (6), (7) and (8), we can get:

$$\rho_X^{gobal}(I)=\min_{t\in I}H(t)-\ \frac{1}{\alpha} \tag{9}$$

$$\rho_X^{local}(t_0)=\min_{t_0\in[M_1\ \ M_2]}H(t_0)-\ \frac{1}{\alpha}=H(t_0)-\frac{1}{\alpha} \tag{10}$$

The Eq. (9) and (10) show that the quantities $\min_{t\in I}H(t)-\ \frac{1}{\alpha}$ and $H(t_0)-\frac{1}{\alpha}$ provide important information concerning the global and local path irregularity of LMSM; moreover, as we already pointed out, $H(t_0)$ is its self-similarity exponent at t_0, and α determines the tail heaviness of its marginal distributions. Eqs. (9) and (10) indicate that $\rho_X^{gobal}(I)$ and $\rho_X^{local}(t_0)$ provide important information about the global and local path irregularity of LMSM. In order to further explain the multifractional characteristics, LMSM paths under $\alpha=1.75$ and three $H(t)$ conditions are simulated, as shown in Fig. 1.

In Fig. 1, the $\rho_X^{gobal}(I)$ of (a), (b) and (c) are equal but the $\rho_X^{local}(t_0)$ is not, which results in the obvious difference of LMSM paths of the three, indicating that local irregularity should be considered in LMSM path description. It is noteworthy that the irregular characteristics of the LMSM path show the same regularity as $H(t)$, i.e. constant, monotone and periodic, which indicates that $\rho_X^{local}(t_0)$ contains all the information of the LMSM path. It can be concluded that when global parameter $\rho_X^{gobal}(I)$ is the same and local parameter $\rho_X^{local}(t_0)$ is different, LMSM paths will still be different. So, introducing local irregularity can describe more actual degradation.

2.2. Non-Gaussian and LRD conditions

For LRD analysis of degraded sequences in real cases, the LRD conditions need to be obtained. Let $t>s>0$, Eq. (2) takes the form:

$$X(t,\ H(t))=\int_0^t\left((t-s)^{H(t)-\frac{1}{\alpha}}-s^{H(t)-\frac{1}{\alpha}}\right)M(ds) \tag{11}$$

In view of Eq. (11) the integrals $\int_0^t\left((t-s)^{H(t)-\frac{1}{\alpha}}-s^{H(t)-\frac{1}{\alpha}}\right)ds$ are finite for all $t\in R$, for $H(t)\neq\frac{1}{\alpha}$. These integrals can be thought of as a time-varying function $b(t)$. $M(ds)$ is a cluster of symmetric Levy stable random variables. In particular, that if $A=\{a_1,a_2,\cdots,a_n\}\in R$ are disjoint Borel sets, then the random variables $M(a_1),\ M(a_2),\cdots,M(a_n)$ are independent. Moreover, for any Borel set $A\in R,t\in R$, the discretized expression of Eq. (11) can be obtained:

$$X(t,\ H(t))=b(t_1)M(a_1)+b(t_2)M(a_2)+\cdots+b(t_n)M(a_n) \tag{12}$$

According to the limit theorem [38]:

$$a_1X_1+a_2X_2+\cdots+a_nX_n\xrightarrow{d}b_nX+c_n \tag{13}$$

where $a_1,a_2,\cdots,a_n$ *and* b_n are non-zero constants, c_n is a real number, the stochastic variables $X_1,X_2,\cdots,X_n$ are independent samples of X, and the symbol $\xrightarrow{d}$ ndicates the same distribution. So, the LMSM is subject to a symmetric Lévy stable distribution; therefore, LFSM has infinite variance, which is, an advantage for representing high-jump data.

The LRD analysis of LMSM is reformatted under the three conditions:

(1) when $H(t)\ =1/\alpha, b(t)$ in Eq. (11) is a constant. According to the central limit theorem, $X(t,\ H(t))$ becomes a Lévy stable motion with independent increments. So $X(t,\ H(t))$ does not have LRD characteristics;

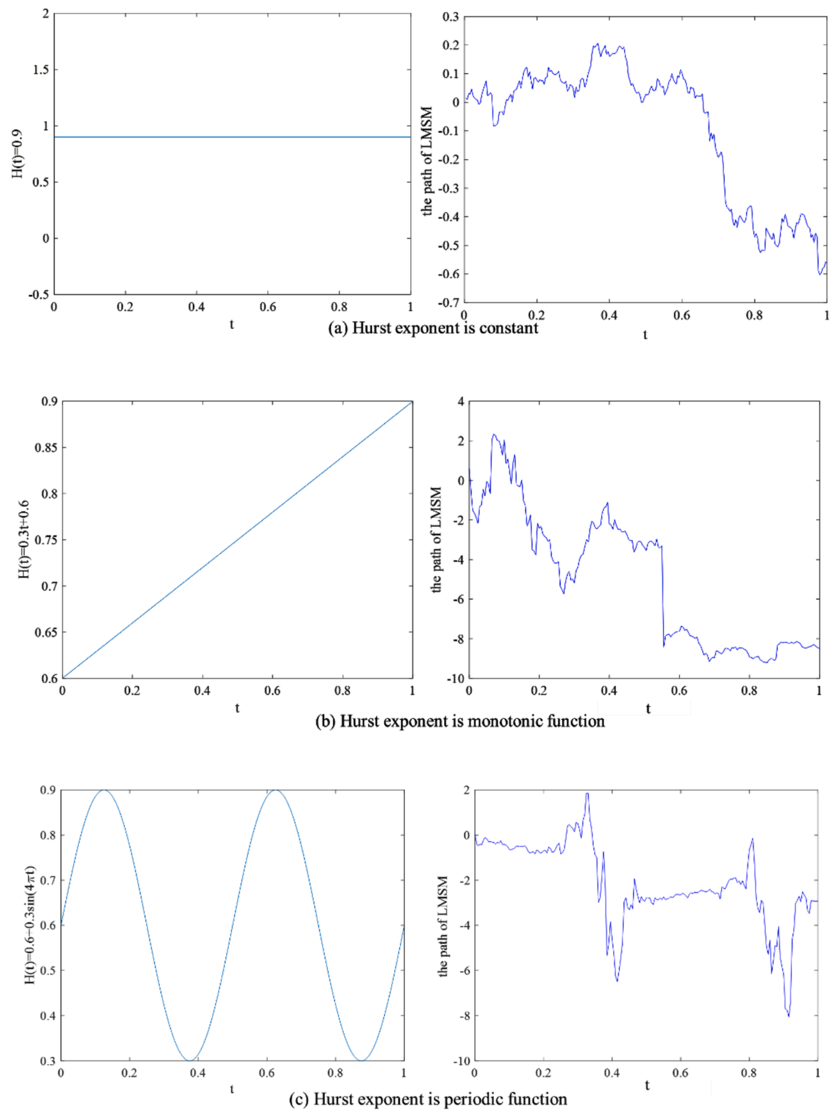

Fig. 1. LMSM paths in case of three Hurst exponent time-varying functions.

(2) when $H(t) < 1/\alpha$, $b(t)$ in Eq. (11) is a time-varying function, but it is inversely proportional to time, and the predicted result will have a negative trend, which results in the actual trend. This situation is called a negative correlation condition;

(3) when $H(t) > 1/\alpha$, $b(t)$ in Eq. (11) is a time-varying function and is proportional to time. So $X(t,\ H(t))$ has LRD characteristics.

In conclusion, the value range of the self-similar index $H(t)$ is (0,1) and combined with the above situation (3), it can be concluded that the LRD condition is:

$$\frac{1}{\alpha} < H(t) < 1 \tag{14}$$

3. Remaining useful life prediction based on LMSM

3.1. Iterative degradation model

In order to consider that the established degradation model has LRD and multifractal characteristics, we adopt the fractal degradation process governed by LMSM $X(t, H(t))$ and nonlinear function $(t;\theta)$. The fractal degradation process $\{Y(t), t \geq 0\}$ is defined as follows:

$$dY(t) = \mu(t;\theta)dt + \delta_a dX(t,\ H(t)) \tag{15}$$

where θ represents the vector of unknown parameters involved in $\mu(t;\ \theta)$ and δ is a diffusion coefficient. The above degradation model is only a general form, and it needs to be discrete and specific to realize simulation. First of all, the incremental distribution form of LMSM, by using Maruyama parameter [40] $dB_t = w(t)(dt)^{1/2}$ is:

$$\int_0^t f(s)(ds)^a = a\int_0^\tau (t-s)^{a-1} f(s)ds \tag{16}$$

and

$$dX = f(t)(dt)^d \tag{17}$$

where d represents the self-similar parameter of random process X. The self-similar function of LMSM is required. self-similar definition is used [39]:

$$x(t) \overset{\Delta}{=} a^{-H} x(at) \tag{18}$$

The derivation process of LMSM's self-similar function is as follows:

$$X(ct,\ H(ct)) = \int_{-\infty}^{ct} \left(a(ct-s)^{H(ct)-\frac{1}{\alpha}} - bs^{H(ct)-\frac{1}{\alpha}}\right)M(ds)$$

$$= c^{H(t)-\frac{1}{\alpha}+\frac{1}{2}} \int_{-\infty}^{t} \left(a(t-s)^{H(t)-\frac{1}{\alpha}} - bs^{H(t)-\frac{1}{\alpha}}\right)M(ds) = c^{H(t)-\frac{1}{\alpha}+\frac{1}{2}}X(t,\ H(t)) \tag{19}$$

Note that the Hurst function does not change with the expansion or contraction of the time scale but is only related to the coarse overpassing of the time sequence itself, so $H(ct) = H(t)$. According to Eqs. (17) and (19), the LMSM increment distribution form can be obtained as follows:

$$dX(t,\ H(t)) = w_\alpha(t)(dt)^{H(t)+\frac{1}{2}-\frac{1}{\alpha}} \tag{20}$$

where $w_\alpha(t)$is white noise subject to Levy stable distribution, i.e. $w_\alpha(t) \sim S_\alpha(0,1,0)$. According to the linear nature of the Levy stable distribution [41]:

$$aX + b \sim S_\alpha(0, |a|\delta, a\mu + b) \tag{21}$$

where a is a non-zero constant and b is a real number. In addition, when Δt is relatively small, it holds that $H(t+\Delta t) - H(t) = o(\Delta t)^{\rho_H}$, i.e. $H(t+\Delta t) = H(t)$. For any $\Delta t > 0$, we have

$$X(t+\Delta t,\ H(t)) - X(t,\ H(t)) \int_{-\infty}^{\infty} \left[(t+\Delta t - s)_+^{H(t)-\frac{1}{\alpha}} - (t-s)_+^{H(t)-\frac{1}{\alpha}}\right]$$

$$+ \left[(t+\Delta t - s)_-^{H(t)-\frac{1}{\alpha}} - (t-s)_-^{H(t)-\frac{1}{\alpha}}\right]M(ds)$$

$$\Rightarrow^{v=s-t} \int_{-\infty}^{\infty} \left[(\Delta t - v)_+^{H(t)-\frac{1}{\alpha}} - (-v)_+^{H(t)-\frac{1}{\alpha}}\right] + \left[(\Delta t - v)_-^{H(t)-\frac{1}{\alpha}} - (-v)_-^{H(t)-\frac{1}{\alpha}}\right]M(dv) = X(\Delta t, H(t)) \tag{22}$$

The LMSM increment distribution can be obtained as follows:

$$X(\Delta t,\ H(t)) \sim S_\alpha\left(0, \Delta t^{H(t)+\frac{1}{2}-\frac{1}{\alpha}}, 0\right) \tag{23}$$

The degradation model (15) is differentiated to obtain iterative degradation prediction model:

$$Y(t+\Delta t) - Y(t) = \mu(\Delta t;\theta)\Delta t + \delta_\alpha w_\alpha(\Delta t)(dt)^{H(t)+\frac{1}{2}-\frac{1}{\alpha}} \tag{24}$$

According to Eqs. (21), (23) and (24), it can be derived:

$$Y(t+\Delta t) - Y(t) \sim S_\alpha\left(\mu(t+\Delta t;\theta) - \mu(t;\theta), \delta_\alpha \Delta t^{H(t)+\frac{1}{2}-\frac{1}{\alpha}}, 0\right) \tag{25}$$

3.2. Algorithm implementation for remaining useful life prediction

Our goal is to predict the RUL of CGC based on the degradation model (25). Similar to existing papers, RUL is defined as the first arrival time when equipment performance degradation to the failure threshold λ. The fault threshold λ is usually determined by prior knowledge. Then the RUL of $\{Y(t), t \geq 0\}$ at time t_f can be defined as [47]:

$$R_f = \inf\{r_f > 0 : Y(t_f + r_f) \geq \lambda | Y(t_f) < \lambda\} \tag{26}$$

According to the Eqs. (21), (23) and (25), we can get:

$$Y(t_f) - \lambda + \delta_\alpha L_{H,\alpha}(r_f) \sim S_\alpha\left(Y(t_f) - \lambda, \delta_\alpha {r_f}^{H(t)+\frac{1}{2}-\frac{1}{\alpha}}, 0\right) \tag{27}$$

For convenience, $Y(t_f) - \lambda + \delta_\alpha L_{H,\alpha}(r_f) = Y(r_f)$. Based on these results, Eq. (31) is rewritten as:

$$R_f = \inf\{r_f : Y(r_f) \geq [\mu(t+\Delta t;\theta) - \mu(t;\theta)] | Y(t_f) < \lambda\} \tag{28}$$

In view of Eq. (28), the RUL is redefined as the first arrival time of symmetric Levy movement to λ. Referents [43,44] propose a spatio-temporal transformation to derive the degradation process with time-varying coefficients to calculate the PDF of the RUL. Since the Levy stable distribution does not have a fixed PDF explicit expression [40], it is a challenge to calculate the PDF of RUL. In order to solve this challenge, Monte Carlo method [45] is used to obtain the PDF of RUL (Fig. 2).

Blue curve in Fig. 2(a) shows the degradation process sequence of the equipment, meanwhile, red curve represents the probability density function of the RUL, which was calculated by using the Monte Carlo method. The identification of degradation state represents the input of the degradation model. (b) represents the specific details of the probability density of RUL calculated based on the Monte Carlo method, where the time corresponding to the maximum value of the probability density distribution curve is the predicted value of RUL. The specific algorithm is as follows:

Step 1: Set the number of Monte Carlo simulations to n, select the prediction starting point t_f, and initialize r_f to 1.

Step 2: Sample a random number L that obeys $S_\alpha\left(Y(t_f) - \lambda, \delta_\alpha {r_f}^{H(t)+\frac{1}{2}-\frac{1}{\alpha}}, 0\right)$.

Step 3: If $L \geq [\mu(t+\Delta t;\theta) - \mu(t;\theta)]$, mark r_f as the RUL, otherwise $r_f = r_f + 1$, and return to Step 2.

Step 4: Count the number of each r_f realization and draw the probability density of the RUL

4. Parameter estimation

The degradation model based on LMSM has constant quantities a, b, c and time-varying parameters $H(t)$. In this work, we estimate the parameters in two steps successively. In the first step, the Hurst function $H(t)$ is estimated by consistent and strongly consistent estimation, which does not require further sharp estimation of covariance. In the second step, the characteristic function method is used to estimate the remaining constant parameters.

4.1. Estimate of $H(t)$

There exist many methods for accurate estimation of the constant Holder exponent of the signal at a given time point. Among them, Scaling range (R/S) method or R/S method and Fourier power spectrum methods are the most widespread [52], which are usually implemented without any prior assumptions about possible scaling behavior in time series. Since these methods are based on linear log-log graphs, resulting in scale exponents of single values, they are not suitable for estimating local time-varying Holder exponents.

In order to have unbiased estimate of low variance, we must consider a local stationary interv al$\tau < |\varepsilon|$, such that $H(t)$ remains constant, i.e., $H(t) = H_t$ for $t \in \left(\frac{t}{2} - \varepsilon, \frac{t}{2} + \varepsilon\right)$. To estimate $H(t)$ over the entire sample path, it is necessary to change the interval according to the local

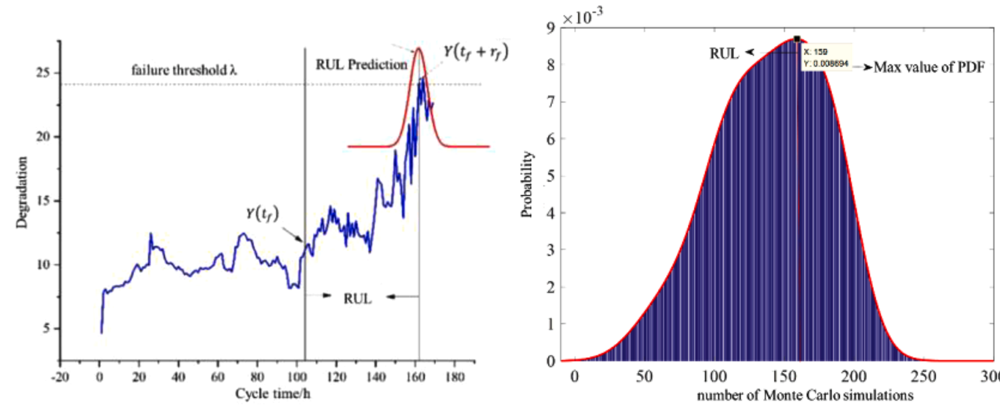

(a) (b)

Fig. 2. RUL prediction based on Monte Carlo method.

regularity of $H(t)$. However, for the sake of simplicity, we make the stationary interval small enough to provide enough k points for a stable estimator. A sequence can be written based on the local growth of an incremental process:

$$S_k(j) = \frac{m}{N-1}\sum_{i=j-k/2}^{j+k/2}|X(i+1,H_t) - X(i,H_t)|\ 1 < k < N \tag{29}$$

where m is the largest integer up to N/k, The expression of local Hurst index $H(t)$ at point $t = j/(N-1)$ is:

$$H_{j/(N-1)} = -\frac{\ln\left[\sqrt{\frac{\pi}{2}}S_k(j)\right]}{\ln(m-1)} \tag{30}$$

Denominator in Eq. (30) has been modified to provide a better estimate for the small sample size of the neighborhood length k. Remember that a smaller value of k will provide better accuracy but will produce greater fluctuations, and vice versa.

4.2. Parameter estimation of the diffusion function

Levy characteristic function [53,54] can be applied to estimate the remaining parameter. It is supposed that the actual degradation $\{y_0, y_1, \cdots, y_n\}$ is obtained by sampling over times $\{t_0, t_1, \cdots, t_n\}$, and the sampling interval is τ. Assume that the degenerate sequence collected by the sub-operator at time interval τ within time t is Y. A degradation difference vector $y_{0:n} = [y_1 - y_0, y_2 - y_1, \cdots, y_n - y_{n-1}]$ is constructed and the ith element in the vector is denoted by $y_{i-1:i}$. According to Eq. (25), $y_{0:n} \sim S_\alpha\left(\mu_i\tau, \delta_a\tau^{H(t)+\frac{1}{2}-\frac{1}{\alpha}}, 0\right)$ is obtained, so position parameter, scale function δ and tail parameter α are estimated as follows:

$$|\gamma(\rho;\alpha,0,\mu,\delta)| = \left|E\left\{e^{j\rho y_{0:n}}\right\}\right| = e^{-\delta|\rho|^\alpha} \tag{31}$$

$$\ln|\gamma(\rho;\alpha,0,\mu,\delta)| = -\delta|\rho|^\alpha \tag{32}$$

Estimation of the scaling function δ:

$$\widehat{\delta} = -\ln|\varphi(1;\alpha,0,\mu,\delta)| = -\ln\left|E\left\{e^{jy_{0:n}}\right\}\right| = -ln\frac{1}{n}\sum_{i=1}^{n}e^{jy_{i-1:i}} \tag{33}$$

Estimation of the tail parameter α:

$$\rho_0^\alpha = \frac{\ln|E\{e^{j\rho_0 y_{0:n}}\}|}{\ln|E\{e^{jy_{0:n}}\}|} = \frac{\ln|\widehat{\varphi}(\rho_0;\alpha,0,\mu,\delta)|}{\ln|\widehat{\varphi}(1;\alpha,0,\mu,\delta)|} \tag{34}$$

$$\widehat{\alpha} = \log_{\rho_0}\left(\frac{\ln|\widehat{\varphi}(\rho_0;\alpha,0,\mu,\delta)|}{\ln|\widehat{\varphi}(1;\alpha,0,\mu,\delta)|}\right) \tag{35}$$

where $\ln|\widehat{\varphi}(\rho_0;\alpha,0,\mu,\delta)| = -ln\frac{1}{n}\sum_{i=1}^{n}e^{j\rho_0 y_{i-1:i}}$. Then, equation (43) takes the form:

$$\widehat{\alpha} = log_{\rho_0}\left(\frac{-ln\frac{1}{n}\sum_{i=1}^{n}e^{j\rho_0 y_{i-1:i}}}{-ln\frac{1}{n}\sum_{i=1}^{n}e^{jy_{i-1:i}}}\right) \tag{36}$$

where $\frac{\ln(2\rho_0)}{{\rho_0}^2-\rho_0} = \widehat{\delta}$. Since the mathematical relationship between the scale function δ and the diffusion coefficient δ_a is $\delta = \delta_a\tau^{H(t)+\frac{1}{2}-\frac{1}{\alpha}}$, the estimated value of the diffusion coefficient δ_a is:

$$\widehat{\delta_a} = \frac{-ln\frac{1}{n}\sum_{i=1}^{n}e^{jy_{i-1:i}}}{\tau^{H+\frac{1}{2}-\frac{1}{\alpha}}} \tag{37}$$

The position parameter μ of the symmetric Lévy stable distribution is estimated by complex number domain of the cumulant generating function of $y_{q_i:q_{i+1}}$:

$$\ln\varphi(\rho;\alpha,0,\mu,\delta) = \delta|\rho|^\alpha + j\left[\delta|\rho|^\alpha\beta\frac{\rho}{|\rho|}\tan\left(\frac{\pi\alpha}{2}\right) + \mu\rho\right] \tag{38}$$

$$\widehat{\mu} = \frac{Im\left\{{\rho_0}^{\widehat{\alpha}}\ln|\widehat{\varphi}(1;\alpha,\beta,\mu,\delta)| - \ln|\widehat{\varphi}(\rho_0;\alpha,\beta,\mu,\delta)|\right\}}{{\rho_0}^{\widehat{\alpha}} - \rho_0} \tag{39}$$

where $\ln|\widehat{\varphi}(\rho_0;\alpha,0,\mu,\delta)| = -ln\frac{1}{k}\sum_{j=1}^{k}e^{j\rho_0 y_{q_i:j}}$, and $\mu = \mu_i\tau$. The drift coefficient μ_i is estimated as follows:

$$\widehat{\mu_i} = \frac{Im\left\{ln\frac{1}{k}\sum_{j=1}^{k}e^{j\rho_0 y_{q_i:j}} - {\rho_0}^{\widehat{\alpha}}ln\frac{1}{k}\sum_{j=1}^{k}e^{jy_{q_i:j}}\right\}}{\tau({\rho_0}^{\widehat{\alpha}} - \rho_0)} \tag{40}$$

5. Case study

The health of the CGC is monitored in real time using data measured by external sensors. Once the interlock value is exceeded, the CGC shuts down. This case study adopts the CGC unplanned shutdown event of Shanghai SecCO Petrochemical Co., LTD. (Model: 11C2000M) occurred on January 8, 2021. The reason for this interlocking is that the seal gas discharge flow indicator (11FI22077) exceeds the interlocking value. Fig. 3 is the process flowchart of CGC low-pressure cylinder with model 11C2000M, and the interlocking source is in the red box.

After analysis and on-site inspection, it was found that the coke scale falling off and attachment on the rotor damaged the dynamic balance (Fig. 4 left), and the inlet and outlet heat exchanger 11E4101N leaked (Fig. 4 right).

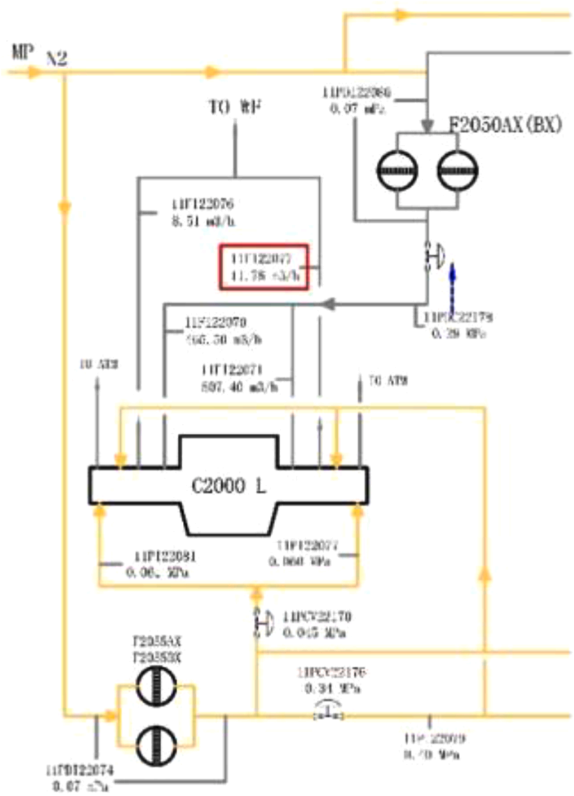

Fig. 3. The Schematic representation of the11C2000M CGC system.

This work establishes a CGC RUL prediction framework, as shown in Fig. 5. First, the data collected by the sensor is screened. The maximum Lyapunov index is used to determine the predictability of the collected data. When the maximum Lyapunov index is greater than 0, the data is predictable [46]. According to the LRD condition $1\ /\alpha\ < H(t) < 1$ deduced in Section 2, the LRD characteristics of the data are judged, filtering out data with both predictability and LRD. Secondly, health indicators are constructed based on the screened data; signal processing techniques are used to construct indicators that are easy to predict. Details of the operation are described below. Thirdly, the health indicator development stage is divided into normal process, degradation process and failure state, and the data in the degradation process were selected for model establishment. Fourth, parameter estimation is reformed, according to Section 4 for specific methods. Fifthly, the establishment of the iterative degradation model is reformed, as described in Section 4.1. Finally, the Monte Carlo method can be applied to calculate the RUL.

5.1. Selection and feature extraction of health indicators

According to the field inspection results (Fig. 4), the root cause of the failure is leakage. In order to prevent leakage, Leakage problems can cause changes in the data measured by the pressure indicator (11PI22001), temperature controller (11TC22154) and liquid level indicator (11LI22052) of the lubricating oil system. resulting in damage to important components, including bearings, and dependent on oil lubrication device.

The time series in Fig. 6-8 are collected every minute from January 6 to January 8, 2021.It can be seen from the Figures that compared with temperature (Fig. 7) and pressure (Fig. 8) parameters, the degradation of liquid level(Fig. 6) is a slow process with an overall upward trend, which can play a role in early warning of incipient failure. However, the liquid level degradation data in Fig. 6 cannot be directly used as a prediction sequence, so feature extraction is required for defining a predictable health indicator. Three commonly used health indicators, Root mean Square [47], Crest Factor [48] and Skip-over Factor [49], are used for feature extraction of the sequence, and the extraction results are shown in Fig. 9. Monotonicity, Robustness, Tradability are used to evaluate the health indicators [47]. Table 1 shows that the skip-over factor sequence is the best.

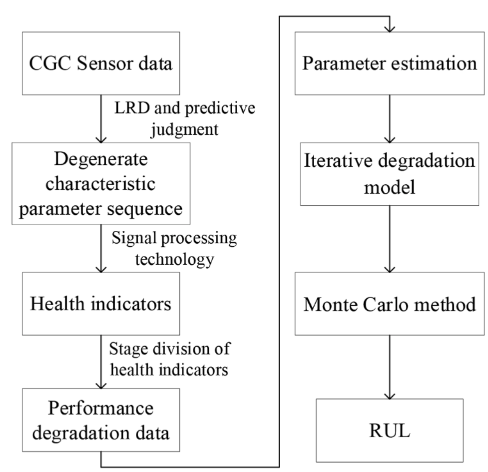

Fig. 5. CGC RUL prediction framework.

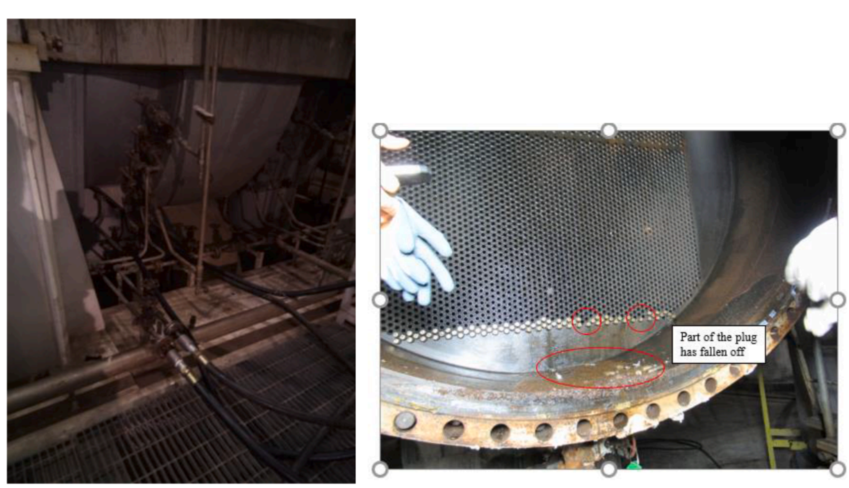

Fig. 4. compressor stopping reason (left: coke off or adhesion in the pressure cylinder; right: plug off inlet and outlet heat exchanger of carbon dihydrogen reactor).

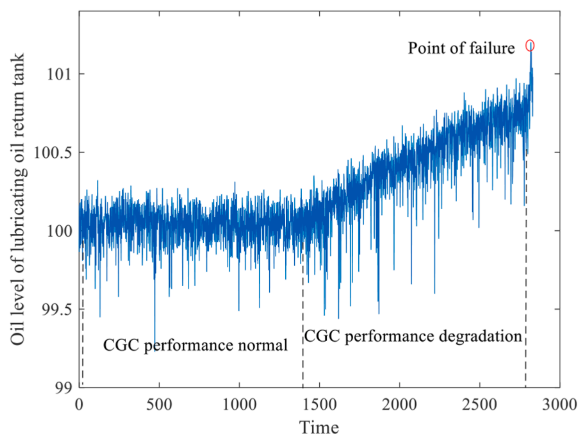

Fig. 6. Time series of liquid level.

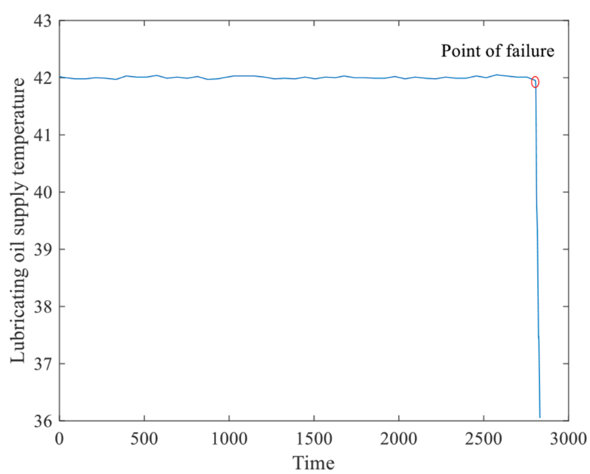

Fig. 7. Time series of temperature.

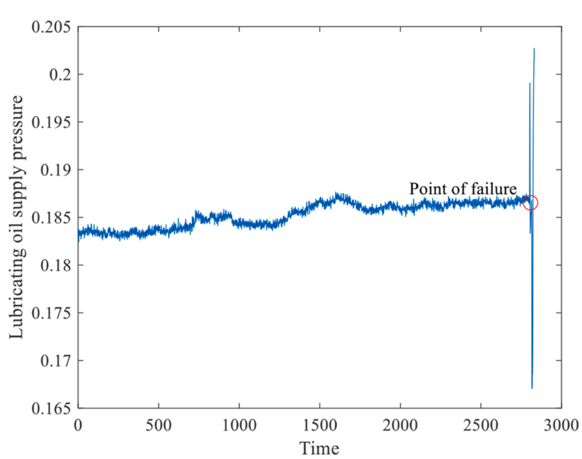

Fig. 8. Time series of pressure parameters.

5.2. Prediction of remaining useful life

Based on the analysis of the degradation data of the CGC lubricating oil level, the degradation process is divided into normal process, degradation process and failure state, as shown in Fig. 6. Here, the RUL of CGC is, then, predicted based on the historical data of the degradation process, that is, the data after 1500.With a preset fault threshold $\lambda = 10$, the LMSM degradation model parameters are estimated under different predicted starting points, Monte Carlo method repetition are 500 times. Table 2 shows the model parameters of the first and last predicted starting points. The PDF of the RUL is shown in Fig. 10.

To show the superiority of the LMSM degradation model, the GC process [20,21], FBM [22,23], LFSM [24,25], and LSTM [26,27] were used as comparison models. Although LSTM has LRD characteristics, it lacks randomness description of degradation process. The Gaussiality of GC process and FBM hardly explains the non-Gaussiality of degradation process. As a comparative model. LFSM has non-Gaussian characteristics, but it

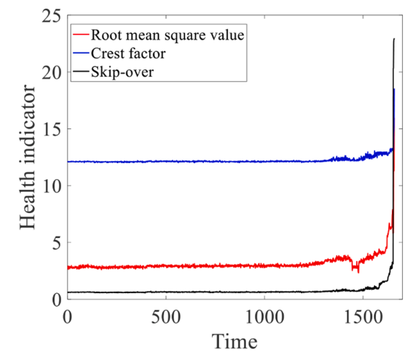

Fig. 9. Characteristic sequence after extraction.

Table 1
Analysis of health indicators.

	Root mean square	Crest factor	Skip-over factor
Monotonicity	0.0595	0.0595	0.0126
Robustness	0.9789	0.9584	0.9958
Trendability	0.5814	0.4082	0.6975
Comprehensive	0.4919	0.4337	0.5828

Table 2
Parameter estimates of the LMSM degradation model.

Prediction starting point	$H(t)$	α	μ	δ
2000	0.6061	1.7024	1.6471	0.2213
2030	0.5990	1.8936	1.7998	0.0531
2060	0.7564	1.7081	1.8706	0.3176
2090	0.6885	1.9602	1.8377	0.0744
2120	0.8362	1.5796	1.8314	0.2365
2150	0.6605	1.8023	1.8717	0.9965
2180	0.6117	1.7345	2.1018	1.2086
2210	0.6058	1.9255	2.4551	1.4217
2240	0.6485	1.7135	2.5335	2.0336
2270	0.7397	1.6865	2.9219	2.0889
2300	0.7405	1.3847	3.0954	2.2604
2330	0.7134	1.4344	3.5832	1.2990
2360	0.7113	1.4997	3.8765	0.6730

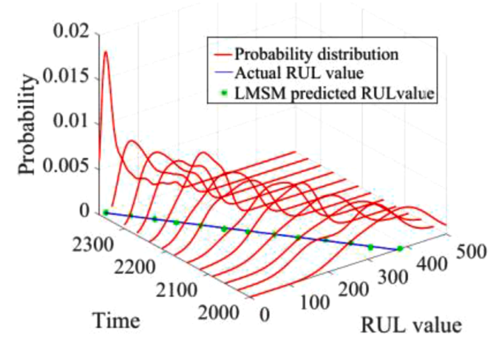

Fig. 10. RUL prediction accuracy of LMSM degradation model.

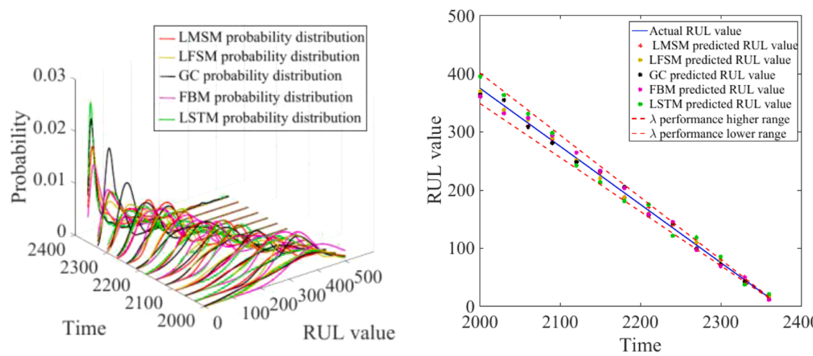

(a) Probability density distribution of RUL prediction (b) RUL prediction for λ=7%

Fig. 11. RUL prediction results for different degradation models. (a) Probability density distribution of RUL prediction (b) RUL prediction for $\lambda = 7\%$.

Table 3
Prediction performance analysis of the different degradation models.

	SOA	HD	RMSE	MAPE
LMSM	0.7662	0.9980	4.9769	0.0259
LFSM	0.7585	0.9973	5.7912	0.0284
GC	0.7480	0.9958	7.2642	0.0385
FBM	0.6325	0.9937	8.8839	0.0499
LSTM	0.4960	0.9858	13.3676	0.0765

is difficult to describe the local irregularity of degradation processes. In comparison with the above models, stochastic and non-Gaussian multifractal features highlight the superiority of the LMSM degradation model. The RUL prediction results of the four methods are shown in Fig. 11.

The results of the four model evaluation indicators (SOA, HD, RSME and MAPE) [50] are given in Table 3.

In comparison with other degradation models, the LMSM degradation model has the smallest RMSE and MAPE, while the SOA and HD values are the largest. Therefore, the accuracy of LMSM degradation model is higher. Then, it can be seen from the analysis of the λ performance area [51] in Fig. 11(b) that the LMSM degradation model also has better prediction accuracy.

6. Conclusion

RUL prediction of equipment with nonlinear, LRD, non-Gaussian and multifractal characteristics in the degradation process is studied in this paper. Compared with the existing models, the degradation model proposed accounts for multifractal features. Multifractal features can explain local irregularity and describe degeneration sequences more realistically.

For its application, a CGC RUL prediction framework is developed, and real data from Shanghai Secco Petrochemical Co., Ltd. is used to verify the validity of the prediction, and compare it with the results of often prediction methods. The error results show that the degeneration model and RUL prediction framework proposed have strong competitiveness.

CRediT authorship contribution statement

Wanqing Song: Writing – review & editing, Writing – original draft, Visualization, Validation, Resources, Methodology. **Shouwu Duan:** Visualization, Software. **Enrico Zio:** Supervision, Methodology. **Aleksey Kudreyko:** Investigation, Formal analysis.

Declaration of Competing Interest

No conflict of interest exists in the submission of this manuscript, and the manuscript is approved by all authors for publication. I would like to declare on behalf of my co-authors that the work described was original research that has not been published previously, and not under consideration for publication elsewhere, in whole or in part. All the authors listed have approved the manuscript that is enclosed. We declare that we have no financial and personal relationships with other people or organizations that can inappropriately influence our work, there is no professional or other personal interest of any nature or kind in any product, service and/or company that could be construed as influencing the position presented in, or the review of, the manuscript entitled.

Acknowledgments

The authors gratefully acknowledge the support of Shanghai SecCO Petrochemical Co., LTD for the provided data. The financial support of this research was provided by the Graduate School of Shanghai University of Engineering Science.

Funding: This research was supported by major project in Ministry of Science and Technology of the People's Republic of China, Grand number: 2020AAA0109301.

References

[1] Li SJ, Li F. Prediction of Cracking Gas Compressor Performance and Its Application in Process Optimization. Chin J Chem Eng 2014;20(6):1089–93. https://doi.org/10.1016/S1004-9541(12)60591-6.
[2] Kwon HJ, Lee D, Lee YK. Failure analysis of blades and vanes of a compressor for a gas turbine engine. Eng Fail Anal 2021;124(3):105386. https://doi.org/10.1016/j.engfailanal.2021.105386.
[3] Jahangiri MR, Fallah AA, Ghiasipour A. Cement kiln dust induced corrosion fatigue damage of gas turbine compressor blades - a failure analysis. Mater Des 2014;62(10):288–95. https://doi.org/10.1016/j.matdes.2014.05.031.
[4] Kryukov II, Shmelev NG, Levchenko AI, Rybnikov AI. Integrated quality control of the rotor discs of gas turbines of gas-compressor units by eddy-current and dye penetrant nondestructive testing. Eng Fail Anal 2016;52(2):102–11. https://doi.org/10.1134/S1061830916020030.
[5] Shlyannikov VN, Ishtyryakov IS. Crack growth rate and lifetime prediction for aviation gas turbine engine compressor disk based on nonlinear fracture mechanics parameters. Theor Appl Fract Mech 2019;103(10):102313. https://doi.org/10.1016/j.tafmec.2019.102313.
[6] X.Y. Zhu, Z.Q. Chen, E. Borgonovo, Remaining-useful-lifetime and system-remaining-profit based importance measures for decisions on preventive maintenance, Reliability Engine -ering and System Safety, 2021, 216(12): 107951. 10.1016/j.ress.2021.107951.
[7] Li F, Lu ZZ, Fang KX. Improved chance index and its solutions for quantifying the structural safety degree under twofold random uncertainty. Reliab Eng Syst Saf 2021;212(10):107635. https://doi.org/10.1016/j.ress.2021.107635.
[8] Zhang ST, Kang R, Liu YH. Remaining useful life prediction for degradation with recovery phenomenon based on uncertain process. Reliab Eng Syst Saf 2021;208(4):107440. https://doi.org/10.1016/j.ress.2021.107440.

[9] Wang W. A model to predict the residual life of rolling element bearings given monitored condition information to date. IMA J Manag Math 2018;13(1):3–16. https://doi.org/10.1093/imaman/13.1.3.

[10] CAI ZY, WANG ZZ. Remaining useful lifetime prediction for equipment based on nonlinear implicit degradation modeling. J Syst Eng Electr 2020;31(1):198–209. https://doi.org/CNKI:SUN:XTGJ.0.2020-01-019.

[11] Liu D, Wang SP, Zhang C, Tomovic M. Bayesian model averaging based reliability analysis method for monotonic degradation dataset based on inverse Gaussian process and Gamma process. Reliab Eng Syst Saf 2018;180(6):25–38. https://doi.org/10.1016/j.ress.2018.06.019.

[12] Lin CP, Ling MH, Cabrera J. Prognostics for lithium-ion batteries using a two-phase gamma degradation process model. Reliab Eng Syst Saf 2021;214(10):107797. https://doi.org/10.1016/j.ress.2021.107797.

[13] Sun F, Li H, Cheng Y. Reliability analysis for a system experiencing dependent degradation processes and random shocks based on a nonlinear Wiener process model. Reliab Eng Syst Saf 2021;215(11):107906. https://doi.org/10.1016/j.ress.2021.107906.

[14] Zheng H, Kong X, Xu H. Reliability analysis of products based on proportional hazard model with degradation trend and environmental factor. Reliab Eng Syst Saf 2021;216(6):107964. https://doi.org/10.1016/j.ress.2021.107964.

[15] Li N, Lei YG, Guo L. Remaining useful life prediction based on a general expression of stochastic process models. IEEE Trans Ind Electron 2017;64(7):5709–18. https://doi.org/10.1109/TIE.2017.2677334.

[16] Sun B, Li Y, Wang Z. An improved inverse Gaussian process with random effects and measurement errors for RUL prediction of hydraulic piston pump. Measurement 2020;173(4):108604. https://doi.org/10.1016/j.measurement.2020.108604.

[17] Huynh KT. An adaptive predictive maintenance model for repairable deteriorating systems using inverse Gaussian degradation process. Reliab Eng Syst Saf 2021;213(10):107695. https://doi.org/10.1016/j.ress.2021.107695.

[18] Wang JJ, Miao YH. Optimal preventive maintenance policy of the balanced system under the semi-Markov model. Reliab Eng Syst Saf 2021;213(9):107690. https://doi.org/10.1016/j.ress.2021.107690.

[19] Wu B, Cui L, Fang C. Reliability analysis of semi-Markov systems with restriction on transition times. Reliab Eng Syst Saf 2019;190(10):106516. https://doi.org/10.1016/j.ress.2019.106516.

[20] Liu H, Song WQ, Zio E. Metabolism and difference iterative forecasting model based on long-range dependent and grey for gearbox reliability. ISA Trans 2021. https://www.sciencedirect.com/science/article/pii/S0019057821002573?dgcid=author.

[21] Liu H, Song WQ, Zhang YJ. Generalized Cauchy Degradation Model with Long-range Dependence and Maximum Lyapunov Exponent for Remaining Useful Life. IEEE Trans Instrum Meas 2021. https://doi.org/10.1109/TIM.2021.3063749.

[22] H. Zhang, D. Zhou, M. Chen, X. Xi, Predicting remaining useful life based on a generalized degradation with fractional Brownian motion, Mechanical Systems and Signal Process, 2019, 115(6): 736–752. 10.1016/j.ymssp.2018.06.029.

[23] Zhang H, Jia C, Chen M. Remaining Useful Life Prediction for Degradation Processes With Dependent and Nonstationary Increments. IEEE Trans Instrum Meas 2021;70(7):3519212. https://doi.org/10.1109/TIM.2021.3085935.

[24] S. Duan, W.Q. Song, E. Zio. Product technical life prediction based on multi-modes and fractional Lévy stable motion, Mechanical Systems and Signal Processing, 2021,161(12):107974. 10.1016/j.ymssp.2021.107974.

[25] Song WQ, Liu H, Zio E. Long-range dependence and heavy tail characteristics for remaining useful life prediction in rolling bearing degradation. Appl Math Model 2022;102(7):268–84. https://doi.org/10.1016/j.apm.2021.09.041.

[26] Liu D, Zhou J, Liao H, Peng Y, Peng X. A health indicator extraction and optimization framework for lithium-ion battery degradation modeling and prognostics. IEEE Transactions on Systems, Man, and Cyber-netics: Systems 2015; 45:915–28. https://doi.org/10.1109/TSMC.2015.2389757.

[27] Fu S, Zhang Y, Lin L. Deep Residual LSTM with Domain-invariance for Remaining Useful Life Prediction Across Domains. Reliab Eng Syst Saf 2021;216(6):108012. https://doi.org/10.1016/j.ress.2021.108012.

[28] Huggins R. Advanced batteries: materials science aspects. New York, NY, USA: Springer Berlin; 2008.

[29] Zhang Z, Si X, Hu C. A prognostic model for stochastic degrading systems with state recovery: application to Li-ion batteries. IEEE Trans 2017;66(4):1293–308. https://doi.org/10.1109/TR.2017.2742298.

[30] Kwon YJ. A Study on the Alkali-aggregate Reaction in High-strength Concrete with Particular Respect to the Blast-furnace Slag Effect. Cement Concrete Res 2005;35(9):1305–13. https://doi.org/10.1016/j.cemconres.2004.09.021.

[31] Zhang HW, Zhou DH, Chen MY, Shang J. FBM-Based Remaining Useful Life Prediction for Degradation Processes With Long-Range Dependence and Multiple Modes. IEEE Trans Reliab 2019;68(3):1021–33. https://doi.org/10.1109/TR.2018.2877643.

[32] Peng W, Li Y-F, Mi J, Yu L, Huang H-Z. Reliability of complex systems under dynamic conditions: a Bayesian multivariate degradation perspective. Reliab Eng Syst Saf 2016;153:75–87. https://doi.org/10.1016/j.ress.2016.04.005.

[33] Fan XP, Vehel JL. Tempered fractional multi-stable motion and tempered multifractional stable motion. ESAIM-Probability Stat 2019;23(5):37–67. https://doi.org/10.1051/ps/2018012.

[34] Ayache A, Hamonier J. Behaviour of linear multifractional stable motion: membership of a critical Holder space. Stochastics-An Int J Prob Stochastics Proc 2017;89(5):709–25. https://doi.org/10.1080/17442508.2016.1276910.

[35] S S, T MS. Stochastic properties of the linear multifractional stable motion. Adv Appl Probab 2004;36(4):1085–115. https://doi.org/10.1142/S0218348x0500.

[36] Bowditch A. Non-Gaussian Fluctuations of Randomly Trapped Random Walks. Adv Appl Probab 2021;53(3):801–38. https://doi.org/10.1017/apr.2020.75.

[37] Yang BH. An Adaptive Filtering Algorithm for Non-Gaussian Signals in Alpha-Stable Distribution. Traitement du Signal 2020;37(1):69–75. https://doi.org/10.18280/ts.370109.

[38] Burnecki K, Wylomanska A, Chechkin A. Discriminating between Light- and Heavy-Tailed Distributions with Limit Theorem. PLoS ONE 2015;10(12): e0145604. https://doi.org/10.1371/journal.pone.0145604.

[39] Zhang ZQ, Xiao YQ. On the Fourier Transforms of Nonlinear Self-similar Measures. J Fourier Anal Appl 2020;26(3):43. https://doi.org/10.1007/s00041-020-09743-9.

[40] Jumarie G. On the representation of fractional Brownian motion as an integral with respect to (dt)a. Appl Math Lett 2004;18(5):739–48. https://doi.org/10.1016/j.aml.2004.05.014.

[41] Liang YJ, Chen W. Reliability analysis for sluice gate anti-sliding stability using Levy stable distributions. Signal Processing 2015;107(9):425–32. https://doi.org/10.1016/j.sigpro.2014.03.044.

[42] Dybiec B, Gudowska-Nowak E, Chechkin A. To hit or to pass it over-remarkable transient behavior of first arrivals and passages for Levy flights in finite domains. J Phys A Math Theor 2016;49(50):504001. https://doi.org/10.1088/1751-8113/49/50/504001.

[43] Roman-Roman P, Serrano-Perez JJ, Torres-Ruiz F. An R package for an efficient approximation of first-passage-time densities for diffusion processes based on the FPTL function. Appl Math Comput 2012;218(17):8408–28. https://doi.org/10.1016/j.amc.2012.01.066.

[44] Zhang H, Chen M, Xi X. Remaining useful life prediction for degradation processes with long-range dependence. IEEE Trans Reliab 2017;66(4):1368–79. https://doi.org/10.1109/TR.2017.2720752.

[45] Lemieux C. Monte Carlo and Quasi-Monte Carlo sampling. New York: Springer; 2009. https://doi.org/10.1007/978-0-387-78165-5.

[46] Li X, Ding R, Li J. Quantitative Comparison of Predictabilities of Warm and Cold Events Using the Backward Nonlinear Local Lyapunov Exponent Method. Adv Atmos Sci 2020;37(9):951–8. https://doi.org/10.1007/s00376-020-2100-5.

[47] Lei YG, Li NP, Guo L. Machinery health prognostics: a systematic review from data acquisition to RUL prediction. Mech Syst Signal Process 2018;104(5):799–834. https://doi.org/10.1016/j.ymssp.2017.11.016.

[48] Dron JP, Bolaers F, Rasolofondraibe L. Improvement of the sensitivity of the scalar indicators (crest factor, kurtosis) using a de-noising method by spectral subtraction: application to the detection of defects in ball bearings. J Sound Vib 2004;270(1–2):61–73. https://doi.org/10.1016/S0022-460X(03)00483-8.

[49] Liu CL, Zhang Y, Sun JR, Cui ZH, Wang K. Stacked bidirectional LSTM RNN to evaluate the remaining useful life of supercapacitor. Int J Energy Res 2021. https://doi.org/10.1002/er.7360.

[50] Yang F, Habibullah MS, Zhang T, Xu Z, Lim P, Nadarajan S. Health index-based prognostics for remaining useful life predictions in electrical machines. IEEE Trans Ind Electr 2016;63(5):2633–44. https://doi.org/10.1109/TIE.2016.2515054.

[51] Wen P, Zhao S, Chen S. A generalized remaining useful life prediction method for complex systems based on composite health indicator. Reliab Eng Syst Saf 2021; 205(1):107241. https://doi.org/10.1016/j.ress.2020.107241.

[52] Barunik J, Kristoufek L. On Hurst exponent estimation under heavy-tailed distributions. Physica A Stat Mech Appl 2010;389(18):3844–55. https://doi.org/10.1016/j.physa.2010.05.025.

[53] Wang XY, Li K, Gao PY. Research on parameter estimation methods for alpha stable noise in a laser gyroscope's random error. Sensors (Basel) 2015;15(8):18550–64. https://doi.org/10.3390/s150818550.

[54] Liu MQ, Han YT, Chen YF, Song H, Yang ZT. Modulation Parameter Estimation of LFM Interference for Direct Sequence Spread Spectrum Communication System in Alpha-Stable Noise. IEEE Syst J 2021;15(1):881–92. https://doi.org/10.1109/JSYST.2020.2991078.